Z. Phys. B – Condensed Matter 75, 265–274 (1989)

Condensed Matter
Zeitschrift für Physik B

Two-dimensional traveling wave patterns in nonequilibrium systems

M. Bestehorn, R. Friedrich, and H. Haken
Institut für Theoretische Physik und Synergetik, Universität Stuttgart, Federal Republic of Germany

Received November 4, 1988

Traveling wave patterns formed at the oscillatory onset of convection in binary mixtures with free slip and permeable horizontal boundary conditions are theoretically derived by means of an order parameter equation for the case of large aspect ratio systems with circular and rectangular geometry. We obtain in addition to 'Zipper states' the so called 'confined states', which so far has been observed only experimentally. Our present study of traveling wave patterns in circular systems, which are the first theoretical investigations in this respect, exhibit a characteristic change of behaviour. Close to onset the waves travel in radial direction towards the sidewalls. For higher Rayleigh-numbers the waves are confined to the circular boundary traveling in azimuthal direction. The occurrence of this transition should be confirmed experimentally.

1. Introduction

If a fluid is heated from below, at a critical temperature gradient convection sets in and results in a stationary regular pattern as is well known from the Rayleigh-Bénard experiment [1]. In contrast, fluid patterns generated in binary mixtures can be either stationary or oscillatory, depending on the value of the separation ratio Ψ, which is related to the concentration ratio of the two mixed fluids [2]. Currently, great effort is devoted to the investigation of the oscillatory instability of convection in binary fluid mixtures [3–8] as a prototype of an oscillatory instability in a large aspect ratio system since it exhibits a great variety of interesting spatio-temporal patterns already close to onset of convection. In narrow fluid containers running convection waves in various forms of traveling roll structures are obtained [5, 6]. Fluid patterns consisting of separate regions with waves running in different directions have been found. Additionally, quasiperiodic fluid motions occur in form of the so-called blinking state [8] consisting of two wave trains running towards the vertical ends of the container. Thereby, the intensities of the wave trains vary periodically in time. Confined states have been observed where the traveling wave motion exists only in a localized region in the container [8]. Recent experiments have been performed with binary mixtures in an annular container. The rolls align radially and travel in an azimuthal diection [7]. Here, also confined convection has been observed.

Numerical simulations of the evolution equation for the spatially slowly varying envelopes of the waves [9] as well as the generalized Ginzburg-Landau equation for an order parameter directly related to the temperature and concentration fields [10] have revealed similar behaviour. Direct numerical simulations of the basic hydrodynamic equations for the two dimensional problem have been performed as well [11]. Experiments in large rectangular and cylindrical vessels exhibit still more complicated spatio-temporal behaviour [3, 12], because of the large number of linearly unstable modes present already close to onset of convection. A theoretical description of spatially slow deformations of traveling waves consisting of nearly aligned rolls have been performed by investigating the evolution equations for the spatially slowly varying envelope function of the waves [13, 14]. The numerical simulation of these evolution equations shows spatial patterns similar to the experimentally [12] investigated 'Zipper state'. Defects and grain boundaries between regions with different orien-

tations of the traveling waves influence the spatio-temporal pattern and are expected [14, 21] to enforce the emergence of three dimensional turbulence.

The evolution equations for the envelope functions (see e.g. [9, 13, 14]) can not be applied to the description of patterns with defects and grain boundaries between regions with traveling waves having different orientations. In order to deal with such problems, where direct numerical simulations are extremely time-consuming due to the fact that the flow is actually three dimensional, we derived the order parameter equation [10]

$$\frac{\partial}{\partial t}\xi(\mathbf{x},t)=(\delta\varepsilon+\lambda_0-\lambda_1\Delta+\lambda_2\Delta^2)\,\xi(\mathbf{x},t) + \iiint d x_1\, d x_2\, d x_3\, A(\mathbf{x}-\mathbf{x}_1,\mathbf{x}-\mathbf{x}_2,\mathbf{x}-\mathbf{x}_3) \cdot\xi(\mathbf{x}_1,t)\,\xi(\mathbf{x}_2,t)\,\xi^*(\mathbf{x}_3,t) \tag{1}$$

for the complex order parameter field $\xi(\mathbf{x}, t)$ which, for the case of convection in binary mixtures, is directly related to the temperature and concentration field in a horizontal two-dimensional plane inside the fluid. We mention that the order parameter field $\xi(\mathbf{x}, t)$ needs not be spatially slowly varying. The order parameter equation (1) is the extension of the equation previously used by Hohenberg and Swift [15], and M. Bestehorn and H. Haken [16] for the description of the nonoscillatory onset of convection in simple fluids to the case of an oscillatory instability. It has also been derived independently by Kawasaki and Ohta [22], but they further reduce the order parameter equation to evolution equations for envelope functions for the amplitudes of left and right traveling waves which are only valid if the convective rolls are aligned nearly parallel.

In this paper, we briefly indicate how the integro-differential equation (1) for the order parameter can be reduced to a partial differential equation: It will turn out that the nonlocal term in (1) may be well approximated by a local one resulting in an order parameter equation which is derived below for the first time. We determine all coefficients of this GGLE for free, permeable or perfect boundary conditions at the upper and lower side of the fluid. We present numerical solutions of the two-dimensional GGLE for large rectangular as well as cylindrical containers describing a three-dimensional fluid motion in a large aspect ratio system. In addition to patterns exhibiting the 'Zipper state' we obtain, for the first time, confined states, which have up to now only been observed experimentally. Our calculations for a cylindrical geometry, which are the first theoretical investigations of traveling waves in circular geometries, show, close to threshold, waves traveling in radial direction from the center to the sidewall of the cell. For larger values of the Rayleigh number, we find a transition to patterns consisting of traveling rolls perpendicular to the sidewall and moving in azimuthal direction. The transition between these two modes of convection is related with an optimization of the Nusselt number, e.g. the heat transport between the two horizontal plates. It would be interesting to confirm the occurrence of this qualitative change of behaviour experimentally.

2. Generalized Ginzburg-Landau-equation

The density of a binary mixture depends on both temperature as well as on concentration. Due to the Soret-effect a local flux of the concentration is induced by a local temperature gradient. As is well-known, the behaviour of the fluid mixture is described by the following four dimensionless parameters: The Rayleigh number R, the separation ratio Ψ, the Lewis number L and the Prandtl number P (see e.g. [2]). For sake of simplicity we shall consider the case of infinite Prandtl-number. Then, the behaviour is mathematically given by the following set of equations for the velocity field $\mathbf{v}(\mathbf{r}, t)$, the temperature field $\Theta(\mathbf{r}, t)$, the pressure $P(\mathbf{r}, t)$, and the concentration $C(\mathbf{r}, t)$:

$$\begin{aligned}
&\Delta\,\mathbf{v}(\mathbf{r},t)+\mathbf{e}_3\,R(\Theta(\mathbf{r},t)-\Psi C(\mathbf{r},t))-\operatorname{grad}P(\mathbf{r},t)=0\\
&\partial_t\,\Theta(\mathbf{r},t)+[\mathbf{v}(\mathbf{r},t)\operatorname{grad}]\,\Theta(\mathbf{r},t)=v_3(\mathbf{r},t)+\Delta\Theta(\mathbf{r},t) \qquad (2)\\
&\partial_t\,C(\mathbf{r},t)+[\mathbf{v}(\mathbf{r},t)\operatorname{grad}]\,C(\mathbf{r},t)\\
&=-v_3(\mathbf{r},t)+L\Delta C(\mathbf{r},t)+L\Delta\Theta(\mathbf{r},t)\\
&\operatorname{div}\mathbf{v}(\mathbf{r},t)=0.
\end{aligned}$$

We assume free boundary conditions for the velocity field $\mathbf{v}(\mathbf{r}, t)$ and fixed concentration on the upper and lower plates. It is well established that oscillatory convection sets in for values of Ψ smaller than $-L^2$.

In a previous paper [10] we described how to derive the GGLE (1) from the basic hydrodynamic equations (2). The nonlocality of the nonlinear interaction term renders a numerical treatment rather time consuming, even in the $2-D$ case. However, a suitable local approximation becomes possible as we shall briefly indicate in the following. For the nonlinear equations (2) we make the ansatz:

$$\begin{aligned}
V_i(\mathbf{r},t)&=\sum_{l=1}^{\infty} d_z f_l(z,\Delta)\,\partial_i\,\Phi_l(\mathbf{x},t)\exp(\mathrm{i}\,\omega_l t)+\text{c.c.},\\
&\qquad i=x,y\\
\begin{bmatrix}V_z(\mathbf{r},t)\\ \Theta(\mathbf{r},t)\\ C(\mathbf{r},t)\end{bmatrix}&=\sum_{l=1}^{\infty}\begin{bmatrix}-\Delta f_l(z,\Delta)\\ g_l(z,\Delta)\\ h_l(z,\Delta)\end{bmatrix}\Phi_l(\mathbf{x},t)\exp(\mathrm{i}\,\omega_l t)+\text{c.c.}
\end{aligned} \tag{3}$$

where Δ denotes the two-dimensional Laplacian. The operators f, g, and h are defined by the linearized problem (2) and the horizontal boundary conditions in accordance with the general derivation of the generalized Ginzburg-Landau-equations given in Chaps. 7 of [17, 18]. We mention that for perfect boundary conditions the z-dependence of these operators can be expressed as $\sin(\pi l z)$. In the following, the unstable modes are denoted by $l=1$. Since all other modes are enslaved by these modes close to instability, $\Phi_1(\mathbf{x}, t)$ will be the order parameter of the system. The complex order parameter $\Phi_1(\mathbf{x}, t)$ describes the spatio-temporal patterns in the horizontal plane. We note that the order parameter field need not be spatially slowly varying. It describes the cellular structure as well as the large scale structures of the patterns in a horizontal plane.

We now make the assumption that the unstable modes Φ_1 couple most strongly to stable modes Φ_s which are slowly varying in $\mathbf{x}$. More precisely, this assumption is equivalent to the approximation

$$\langle \mathbf{v}(\mathbf{r}, t)\, \nabla \Theta(\mathbf{r}, t)\rangle \simeq \mathbf{v}(\mathbf{r}, t)\, \nabla(\Theta(\mathbf{r}, t)-\langle\Theta(\mathbf{r}, t)\rangle)$$
$$\langle \mathbf{v}(\mathbf{r}, t)\, \nabla C(\mathbf{r}, t)\rangle \simeq \mathbf{v}(\mathbf{r}, t)\, \nabla(C(\mathbf{r}, t)-\langle C(\mathbf{r}, t)\rangle) \qquad (4)$$

where the brackets indicate a spatial average over the horizontal plane of the fluid layer. This approximation and the adiabatic approximation allow us to express the slaved modes by the order parameter:

$$\Phi_s(\mathbf{x}, t)=a\,|\nabla\Phi_1(\mathbf{x}, t)|^2+b\,|\Phi_1(\mathbf{x}, t)|^2 + c(\nabla\Phi_1(\mathbf{x}, t))^2+d\,\Phi_1(\mathbf{x}, t)^2. \qquad (5)$$

The constants a, b, c, and d can be determined explicitely from the basic equations in a well-known manner (see Chap. 7 of [18]). We finally arrive at the generalized Ginzburg-Landau-equation for $\Phi_1(\mathbf{x}, t)$. (Here and in the following we suppress the index 1 at the order parameter Φ.)

$$\partial_t \Phi(\mathbf{x}, t)=(\delta\varepsilon+\lambda_0-\lambda_1\Delta+\lambda_2\Delta^2)\,\Phi(\mathbf{x}, t) -\alpha\Phi(\mathbf{x}, t)\,|\Phi(\mathbf{x}, t)|^2-\beta\Phi(\mathbf{x}, t)\,|\nabla\Phi(\mathbf{x}, t)|^2 -\gamma\Phi^*(\mathbf{x}, t)(\nabla\Phi(\mathbf{x}, t))^2. \qquad (6)$$

We computed the coupling coefficients α, β, and γ for perfect boundary conditions. We mention that there exists a relation between these coefficients and the coefficients A, B obtained from the generalized Ginzburg-Landau-equations (see Eq. (3) of [10]) for the case of an instability with modes with a single wave number k_c. They read:

$$A=\alpha+\beta k_c^2-\gamma k_c^2$$
$$B=3\alpha+\beta k_c^2+\gamma k_c^2. \qquad (7)$$

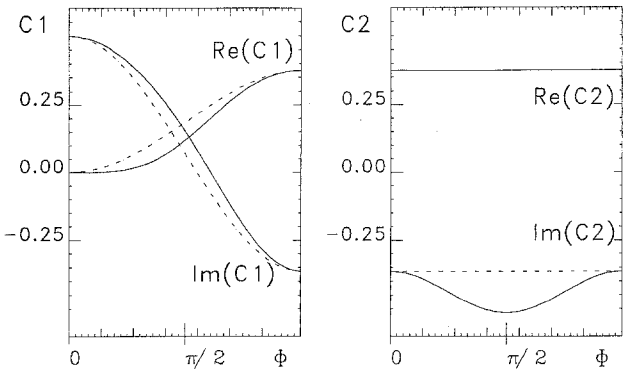

Fig. 1. The nonlinear coupling coefficients $C_1(\phi)$ and $C_2(\phi)$ as functions of the angle ϕ calculated from the basic hydrodynamic laws (solid lines) and their approximate values using the nonlinearity of (6) (dotted lines)

The numerical results presented in the next two sections are based on the values for α, β, and γ for perfect boundary conditions. The corresponding expressions for A and B can be found in [10].

The approximation made in (6) for the slow spatial variation of Φ_s can be justified in the following way: we compared the angular dependence of the coupling strength of two plane waves with a certain direction of propagation with that which can be obtained by means of amplitude equations. If we restrict ourselves on $|k|=|k_c|$, the amplitude equations can be cast into the form:

$$\partial_t \xi(\mathbf{k}, t)=\lambda(k^2)\,\xi(\mathbf{k}, t)-\int_0^{2\pi} \mathrm{d}\phi\; C_1(\phi)\,\xi(\mathbf{k}, t)\,|\xi(\mathbf{k}_1, t)|^2 - \int_0^{\pi} \mathrm{d}\phi\; C_2(\phi)\,\xi(-\mathbf{k}, t)^*\,\xi(\mathbf{k}_1, t)\,\xi(-\mathbf{k}_1, t). \qquad (8)$$

The angle ϕ is defined as the angle between the wave vectors $\mathbf{k}$ and $\mathbf{k}_1$ with absolute value k_c. $\xi(\mathbf{k})$ denotes the slowly varying amplitude function of a plane wave with wave-vector $\mathbf{k}$. We have calculated the functions $C_1(\phi)$ and $C_2(\phi)$ from the basic hydrodynamic equations for convection in binary mixtures using again free/free horizontal boundary conditions for the velocity field. The results compared to those obtained from the GGLE (6) are shown in Fig. 1. We obtain a sufficiently good approximation especially for the vicinity of $\phi=0$, $\phi=\pi$. Therefore, Eq. (6) reflects the interaction between traveling waves ($\phi=0$) and standing waves ($\phi=\pi$) exactly.

Furthermore, the nonlinear interaction between waves with different orientations is sufficiently well reproduced without any qualitative difference. It is obvious that the inclusion of nonlinear terms of the

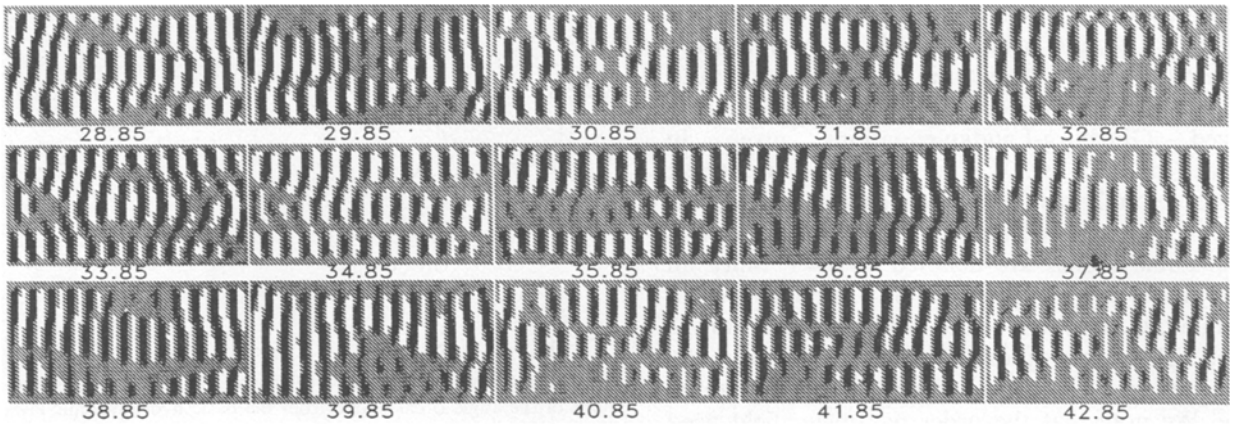

Fig. 2. Traveling wave patterns in a rectangular container with aspect ratio 36:18:1. (Separation ratio $\psi = -0.5$, $\varepsilon = 0.035$)

form $\Phi \partial_{x_i} \partial_{x_j} \Phi \partial_{x_i} \partial_{x_j} \Phi^*$ may be used to improve the approximation of the angular dependence in (6).

The order parameter equation (6) describes the spatio-temporal evolution of a scalar field which is directly related to the hydrodynamic variables. Therefore it is straightforward to specify boundary conditions. If we require vanishing velocity components on the sidewalls as well as vanishing disturbances of the linear temperature and concentration profiles, Eq. (3) yields:

$$\Phi(\mathbf{x}, t) = \mathbf{n} \nabla \Phi(\mathbf{x}, t) = 0. \tag{9}$$

The boundary conditions (6) are correct up to the order of $\varepsilon^{1/2}$, where ε is the reduced Rayleigh number $(R - R_c)/R_c$.

We mention that experiments with realistic boundary conditions yield, for small values of Ψ, a slightly subcritical bifurcation. In the present case of free/free horizontal boundary conditions the bifurcation turns out to be supercritical, which is a result of the finite size of the container in horizontal directions. As is well-known periodic boundary conditions in horizontal directions do not, in the approximation of the nonlinear terms up to third order in the amplitudes, lead to a saturation of the traveling waves (the real part of the coefficient A of (3) of [10] vanishes). This result however, turns out to be irrelevant for finite size containers since the effects of the vertical boundaries are not restricted to a small boundary layer but effects the amplitude of the unstable modes considerably also in the bulk, as can be seen in Fig. 3 of [10]. In our opinion the question of a sub- or supercritical transition is not of major importance with respect to the problem of pattern formation. It seems to be more important to find an accurate description of the nonlinear interaction between waves with different orientations. This has been achieved by the order parameter equation above given for free/free horizontal boundary conditions.

3. Numerical results

In order to investigate the spatio-temporal behaviour of a fluid described by (6), we applied a semi-implicit one-step forward time integration method. The rectangular geometry was approximated by a rectangular mesh with 64×128 grid points. The circular geometry was approximated by a quadratic mesh with 128×128 grid points. For a radius of 18, this corresponds to about 10 meshpoints per critical wavelength which gives a reasonable spatial resolution. The inversion of the linear differential operator in (6) was achieved by a fast Fourier-transform. The nonlinearities were computed in the configuration space using a finite difference scheme. The boundary problem results in an inhomogeneous set of linear equations at each time step, which was solved by an iteration method. The time step in the scaling of (6) was choosen with 0.03, the program was implemented on a DEC-VAX 8300 and needs about 25 s process time per time-step for the quadratic mesh. This gives us the possibility to calculate relatively long evolution-series with an appropriate time resolution in a reasonable CPU-time.

In the case of rectangular fluid containers the rolls of the traveling waves are nearly aligned perpendicular to the larger side of the container. Waves traveling to the left are located at the left hand side and waves traveling to the right at the opposite side. In contrast to the nonoscillatory Bénard-problem [16, 19] the rolls need not be perpendicular to the boundary since the waves can be reflected. For small values of the reduced Rayleigh number ε (see Fig. 2) the spatial structure along the rolls is only slightly disturbed, but, nevertheless, there are periods where the spatial patterns exhibit the Zipper state (see Fig. 2, e.g. the pattern at $t = 34.85$). For higher values of ε the traveling waves show the tendency to be confined to localized regions (see Fig. 3). The existence of confined

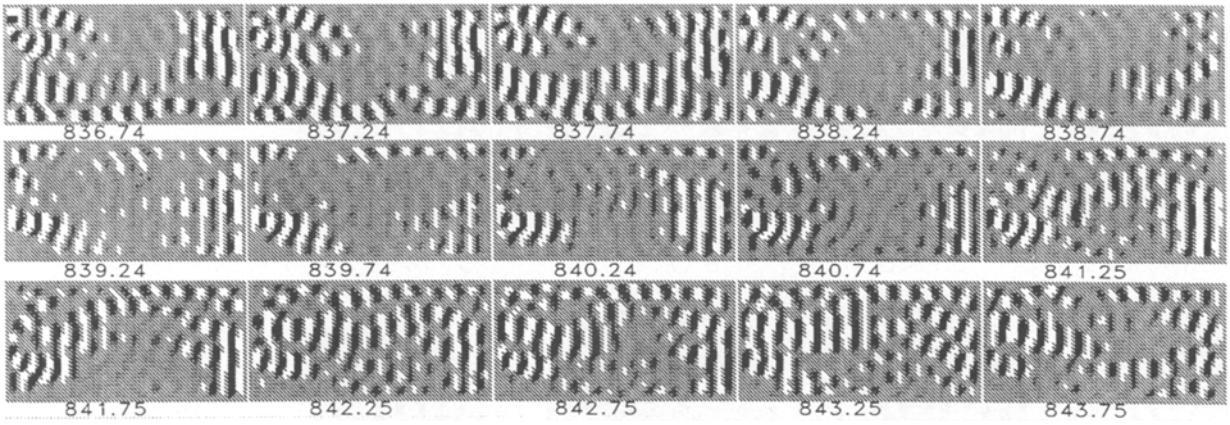

Fig. 3. Traveling wave patterns in a rectangular container with aspect ratio 36:18:1. (Separation ratio $\psi = -0.5$, $\varepsilon = 0.05$)

states is a major result of the experimental investigations of oscillatory convection in binary fluids [3–7].

The calculations for circular geometries were started with two different initial conditions at $t=0$: First, we used a random-dot pattern (RD), second an initial pattern of concentric rolls (CR) with wavelength $\lambda = 2\pi/|k_c|$, where k_c has the value of the critical wave-vector for perfect boundary conditions. The separation ratio and the Lewis number were fixed at $\Psi = -0.5$, $L=0$ for all runs, ε was varied in the range from 0.025 to 0.05. Due to the finite geometry of the container, convection does not set in at $\varepsilon=0$ but at a small positive value, which decreases with increasing aspect ratio. From a linear analysis (see Sect. 4) we calculated the shift of onset as $\varepsilon_s = 0.024$. This shift was confirmed by the numerics. Directly above ε_s the patterns for RD-condition become strongly time-dependent and consist of modes with a weak angular dependence (low values of m, see Fig. 6, part 4). The direction of propagation of the wave is dominated by a more or less concentric movement from the center to the sidewalls (Fig. 4a). This holds also for a CR-initial condition. Here, initially the concentric arrangement of the rolls is conserved for times long compared to the vertical diffusion-time (Fig. 4b), although additional oscillations connected with a non-axisymmetric spatial deformation are superimposed on the regular concentric traveling wave rolls. In the center of the circular container, the fluid patterns consist of standing waves with frequency ω_c. Close to the sidewall the rolls exhibit more and more traveling-wave character. It is quite interesting to note that different initial conditions may lead, at the same values of the control parameters, to coherent patterns (CR-initial condition) and to irregular spatial patterns (RD-initial condition). Although it can not be decided wether the two apparently different behaviours still last for very long times we see that defects generated by the RD-initial conditions prohibit, at least for a very long time, the fluid to settle down to the more coherent spatial structures obtained for CR-initial conditions. The importance of defects for the generation of spatially irregular patterns has been emphasized by P. Coullet et al. [14, 21].

A quite different behaviour occurs for slightly larger ε: At $\varepsilon > 0.027$, the waves start to travel in azimuthal direction with a slightly lower frequency than the critical one and the rolls have the tendency to align perpendicularly to the boundary. The fluid in the center remains nearly at rest (Fig. 5a, RD-condition), a pattern which is reminiscent of the confined states. Wave trains with a spiral structure occur close to the center traveling towards the outer boundary. To demonstrate that the rotating pattern with spiral structure for somewhat larger ε is independent from the initial conditions, we repeated the last run for the CR-initial values. The result is shown in Fig. 5b. We mention that the direction of rotation is purely random and established by symmetry breaking.

4. Mode analysis for oscillatory convection in circular geometries

In order to gain deeper insight into the qualitative transition between radially and spirally traveling waves reported in the last section, it is necessary to make a more detailed investigation of the order parameter equation (6) for a circular geometry with the boundary conditions (9). The eigenfunctions of the linear operator in cylindrical coordinates can be represented as

$$\eta_m(r, \phi) = A(t)[a_1 B_m(k_1 r) + a_2 B_m(k_2 r)] \cdot \exp(i(m\phi + \omega_c t)). \tag{10}$$

Here, B_m are the Bessel-functions of the first kind of the m-th order. The sign of m defines the direction

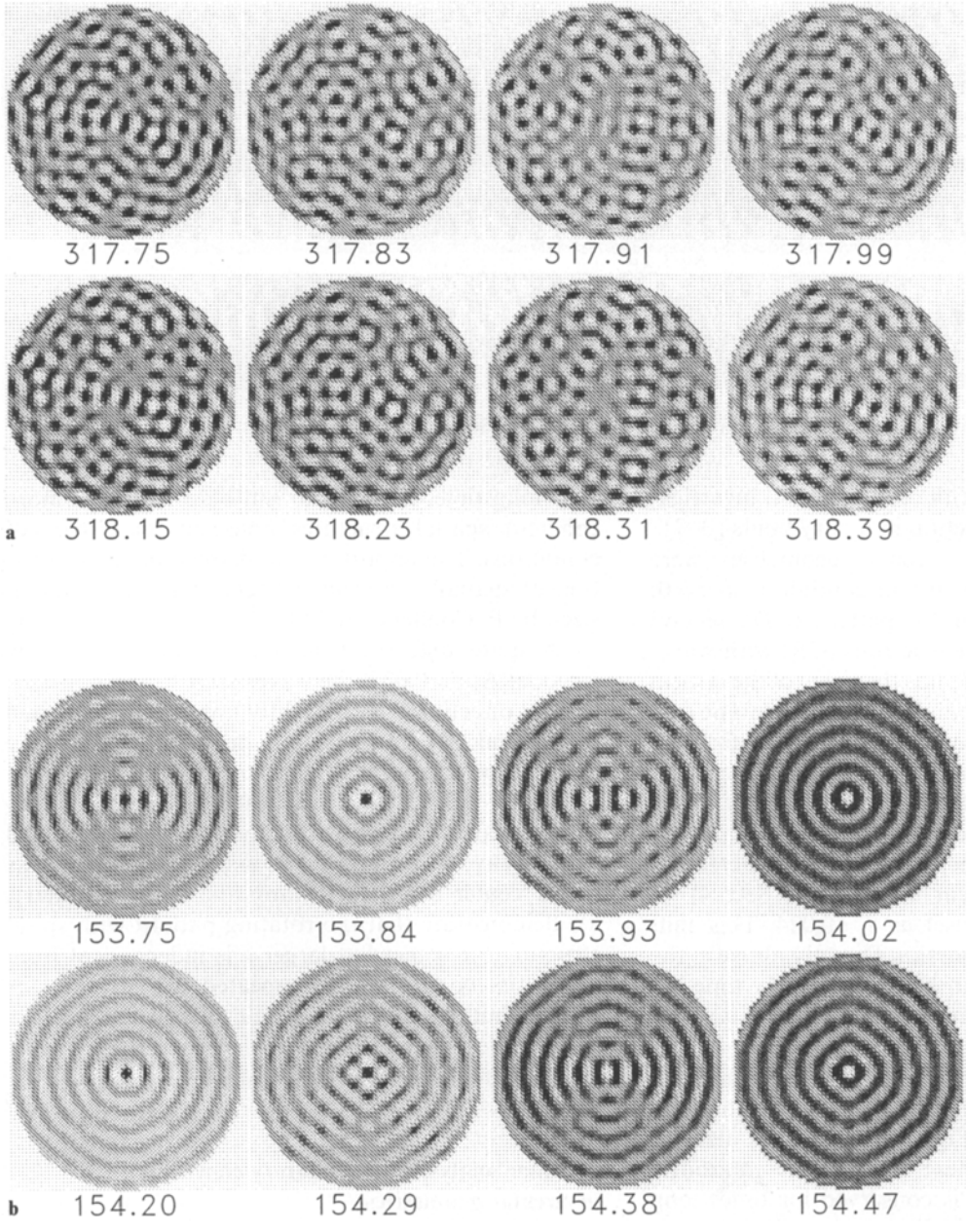

Fig. 4a and b. Temporal evolution of traveling wave pattern in a circular box with diameter 36. (Separation ratio $\psi = -0.5$, $\varepsilon = 0.025$). **a** RD-initial conditions: The patterns consist of several wave trains running towards the boundary. The spatial pattern is irregular. **b** CR-initial conditions: The pattern consists of wave trains running towards the boundary. The pattern is spatially coherent

of propagation in azimuthal direction of the pattern. For positive m, the pattern rotates clockwise and the corresponding amplitude will be denoted with $A_R(t)$. $A_L(t)$ describes a counterclockwise rotation for $m<0$. The values of k_i and a_i in (12) are fixed by the boundary conditions and the following characteristic polynomial:

$$\lambda_0 + \lambda_1 k^2 + \lambda_2 k^4 = \Lambda. \tag{11}$$

In order to compute k_i and the eigenvalues Λ which belong to $\varepsilon = 0$ in Eq. (6) we applied a complex regula-falsi-method. The real part of Λ reflects the shift of the critical point due to the finite geometries and depends therefore on the radius R of the container. Figure 6 shows six basic fluid patterns for several positive values of m (mode 0-32). Since $\omega_c > 0$, they rotate clockwise. The modes with large values of m describe fluid motions more and more confined to the circular boundary. Due to the large aspect ratio of the geometry the modes have roughly the same linear growth rate and nonlinear mode selection becomes significant for the process of pattern formation. A degeneracy

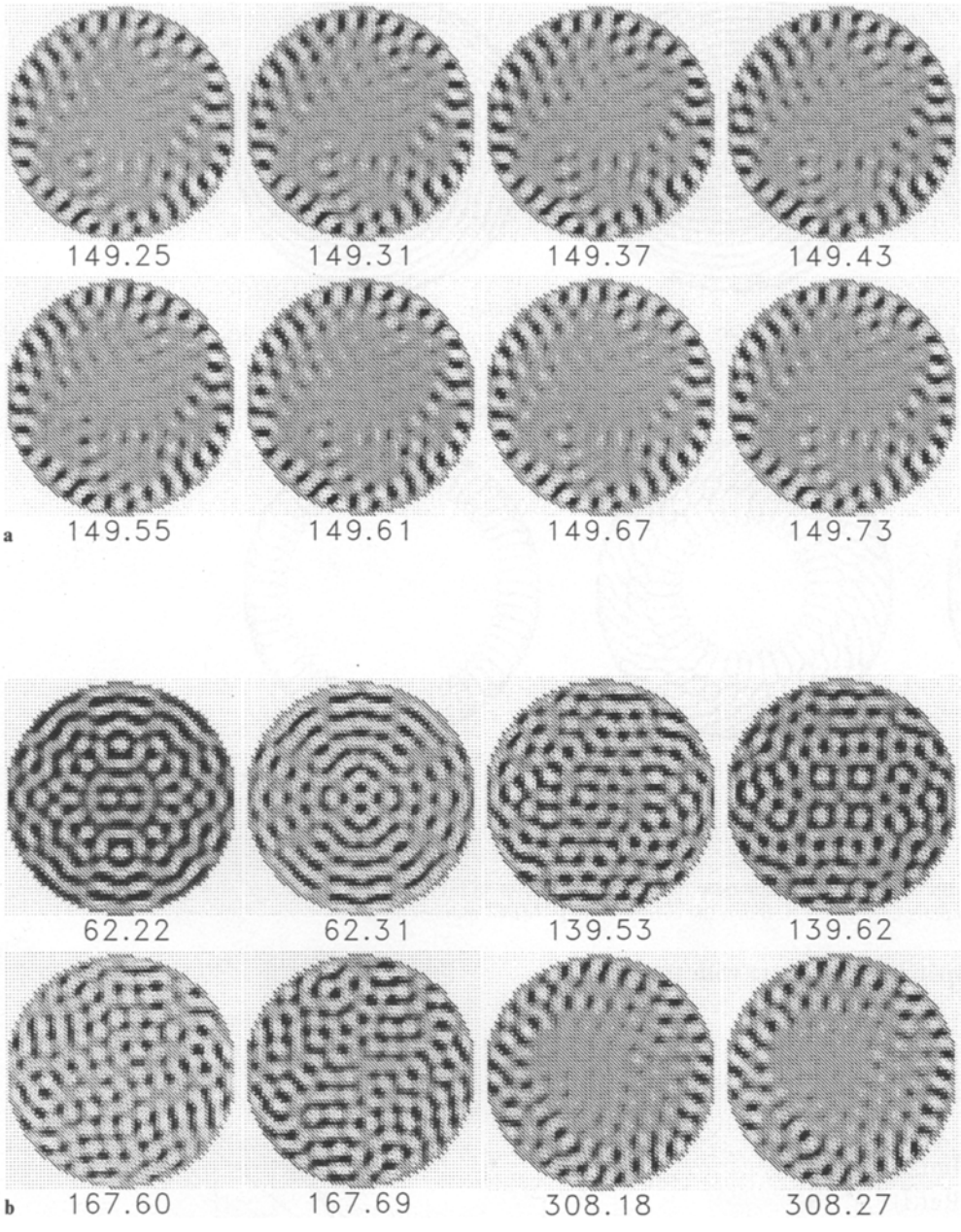

Fig. 5a and b. Temporal evolution of traveling wave pattern in a circular box with diameter 36. (Separation ratio $\psi = -0.5$, $\varepsilon = 0.03$). **a** RD-initial conditions: The final pattern consists of convective motions confined to the circular boundary. The waves travel in azimuthal direction. **b** CR-initial conditions: The final state is independent from initial conditions

originates due to the $O(2)$ symmetry of the circular geometry. If we assume that only the modes with m and $-m$ are excited, then the resulting amplitude equations take the form

$$\begin{aligned} d_t A_L(t) &= [\delta\varepsilon + \Lambda] A_L(t) \\ &\quad + [\tilde{A}|A_L(t)|^2 + \tilde{B}|A_R(t)|^2] A_L(t) \\ d_t A_R(t) &= [\delta\varepsilon + \Lambda] A_R(t) \\ &\quad + [\tilde{A}|A_R(t)|^2 + \tilde{B}|A_L(t)|^2] A_R(t) \end{aligned} \tag{12}$$

where A_L, A_R denote the amplitudes of the clockwise and counterclockwise rotating patterns. The coefficients $\tilde{A}$ and $\tilde{B}$ can be calculated in a straightforward manner by inserting (10) in (6). It turns out that the absolute value of $\mathrm{Re}(\tilde{A})$ is always larger than that of $\mathrm{Re}(\tilde{B})$. Linear stability analysis of (12) shows that under this condition a coexistence of A_L and A_R becomes impossible, i.e. a superposition of clockwise and counterclockwise rotating patterns forming a standing wave pattern in azimuthal direction does

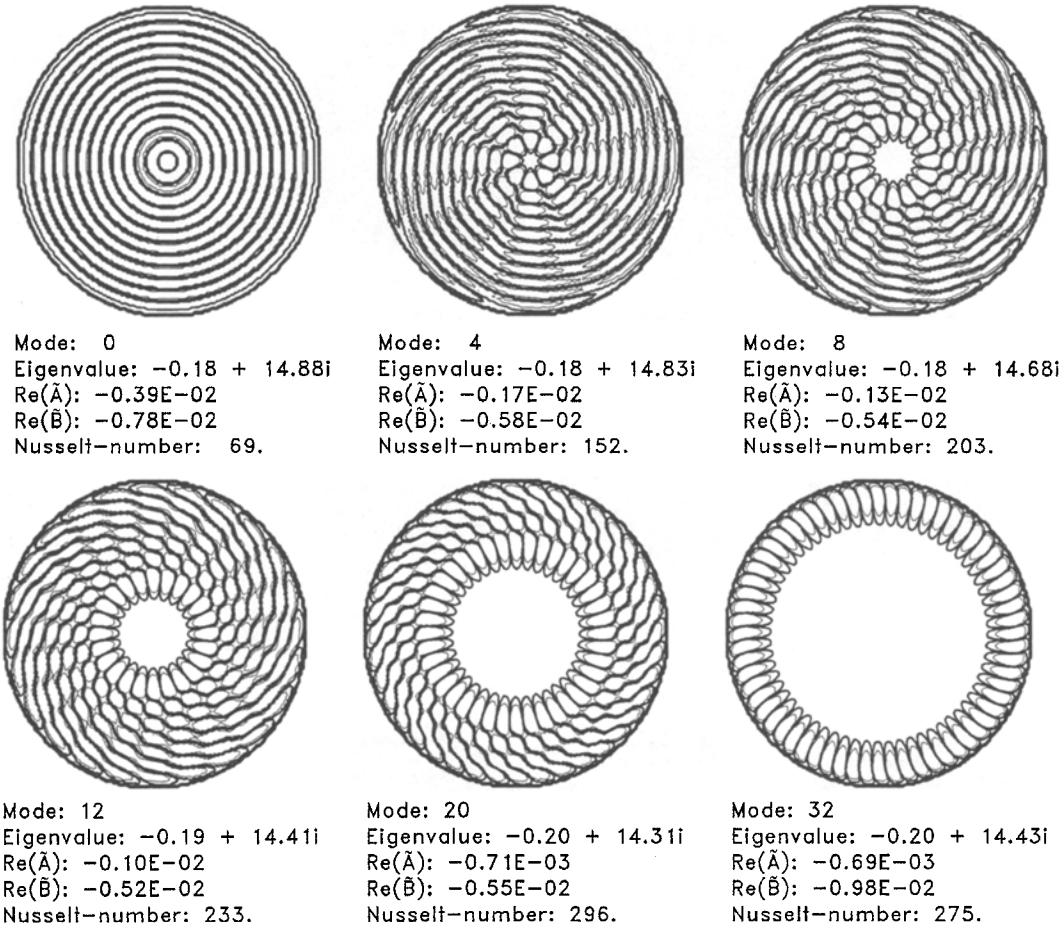

Fig. 6. Convective patterns corresponding to the eigenmodes of the linear operator of (6) for different values of m with the corresponding eigenvalue and the nonlinear coupling coefficients $\tilde{A}$, $\tilde{B}$ and the corresponding Nusselt number ($\varepsilon = 0.05$)

not occur. Therefore, the pattern will rotate with the amplitude

$$|A_{L,R}|^2 = -\frac{\delta\varepsilon + \mathrm{Re}(\Lambda)}{\mathrm{Re}(\tilde{A})} \tag{13}$$

and the angular velocity

$$\Omega = \pm\left[-\omega_c/m - \mathrm{Im}(\Lambda) + \frac{\mathrm{Im}(\tilde{A})}{\mathrm{Re}(\tilde{A})}\,\mathrm{Re}(\Lambda)\right]. \tag{14}$$

Why does the transition between radially and spirally traveling waves observed in part 3 occur for increasing ε? A possible explanation lies in the behaviour of the heat flux through the fluid layer by the selected mode. In order to examine the contribution of convection to the heat flux we calculated the Nusselt numbers corresponding to the modes (10) with the amplitudes (13) as a function of ε. The Nusselt number is given by

$$Nu_m = 1 + 2\pi \int_0^R r\,\mathrm{d}r\,|\eta_m(r,\phi)|^2. \tag{15}$$

It increases linearly with ε. It turns out that the increase of Nu_m of those modes with a smaller ε-shift

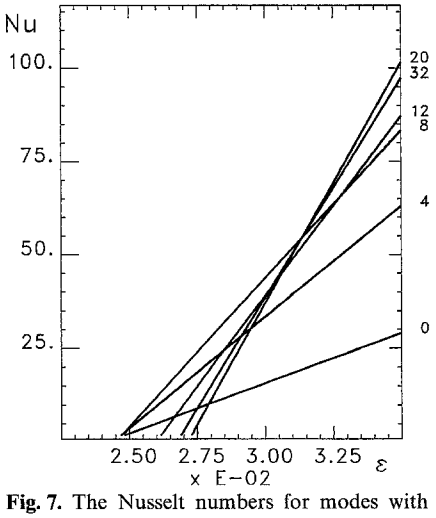

Fig. 7. The Nusselt numbers for modes with several values of m as functions of the reduced Rayleigh number ε

(modes with small absolute values of m) is smaller than the increase of the heat flux of the modes which become unstable at larger ε (modes with larger absolute values of m). Figure 7 demonstrates the dependence of the Nusselt numbers on ε for the basic pat-

terns shown in Fig. 6. We conclude that the qualitative change between radially and azimuthally traveling wave patterns is related to the optimization of the heat flux from the following facts: The numerically obtained patterns are, close to onset apparently formed by modes with small absolute values of m (see especially Fig. 4a). The confined patterns at larger values of the Rayleigh number consist of modes with large absolute values of m. The patterns are therefore mainly determined by these modes, which maximize the heat transport.

6. Conclusion

In the present paper we used the generalized Ginzburg-Landau-equation for an order parameter derived from the $3D$ hydrodynamic basic equations in order to describe the spatio-temporal behaviour of a binary mixture in the oscillatory regime. Results, which are, to the best of our knowledge, presented here for the first time, are the following: a) The generalized Ginzburg-Landau equation (1) has been shown to take, in a well defined approximation, the form of (6) for the case of convection in binary mixtures with free/free and permeable horizontal boundary conditions. We integrated the generalized Ginzburg-Landau equation for rectangular as well as circular geometries with large aspect ratios. b) In the case of rectangular containers we found, in addition to patterns exhibiting the 'Zipper state', confined states, which have so far only been observed experimentally. c) In the case of large circular containers we found a qualitative change in the behaviour of the fluid patterns. Close to threshold the patterns consist of traveling waves, which move in a more or less concentric way from the center of the fluid container to the sidewall. Above the transition, the pattern changes to rolls aligned perpendicular to the sidewalls and running in azimuthal direction with a somewhat lower frequency than the critical one. d) By a normal mode analysis of (6) we have shown by a calculation of the corresponding Nusselt numbers that the observed transition optimizes the contribution of convection to the heat flux between the horizontal plates.

In conclusion we point out that the present investigations of the onset of oscillatory convection in binary mixtures by means of an order parameter equation has allowed us to calculate three-dimensional traveling wave patterns in large aspect ratio systems. The patterns are quite similar to patterns which have already been obtained experimentally (however in systems with different boundary conditions). Additionally, in large circular containers we found a characteristic transition between radially traveling waves (low Rayleigh numbers) and waves confined to the outer boundary traveling in azimuthal direction. It would be interesting to verify this transition experimentally and to study the impact of rigid/rigid and impermeable horizontal boundary conditions on this transition.

From the theoretical point of view, it would be interesting to include terms in the GGLE which become important if the Prandtl number is very low, say $P \ll 1$. The GGLE for this region has to be extended by adding an equation for the generation of a horizontal vorticity field as first discussed for pure fluids by Siggia et al. [20]. That extension should allow a better comparison with experiments in He-mixtures or in gases.

We gratefully acknowledge useful discussions with T. Grauer, K. Scheller, A. Wunderlin, K. Marx, H. Ohno, A. Fuchs, and B. Hölle. We wish to thank the Volkswagenwerk foundation, Hannover, for financial support within its project on Synergetics.

References

1. Busse, F.H.: Rep. Prog. Phys. **41**, 1929 (1978)
2. Platten, J.K., Legros, J.C.: Convection in liquids. Berlin, Heidelberg, New York: Springer 1983
3. Steinberg, V., Moses, E., Fineberg, J.: Proceedings of the International Conference on 'The Physics of Chaos and Systems Far From Equilibrium', Monterey, Jan 10–14, 86. Nucl. Phys. (Proc. Suppl.) B **2**, 109 (1987)
4. Kolodner, P., Passner, A., Williams, H.L., Surko, C.M.: Proceedings of the International Conference on 'The Physics of Chaos and Systems Far From Equilibrium', Monterey, Jan 10–14, 86. Nucl. Phys. (Proc. Suppl.) B **2**, 97 (1987)
5. Heinrichs, R., Ahlers, G., Cannell, D.S.: Phys. Rev. A**35**, 2761 (1987)
6. Ahlers, G., Cannell, D.S., Heinrichs, R.: Nucl. Phys. (Proc. Suppl.) **B2**, 77 (1987)
7. Kolodner, P., Bensimon, D., Surko, C.M.: Phys. Rev. Lett. **60**, 1723 (1988)
8. Fineberg, J., Moses, E., Steinberg, V.: Phys. Rev. Lett. **61**, 838 (1988)
9. Cross, M.C.: Phys. Rev. Lett. **57**, 2935 (1986)
10. Bestehorn, M., Friedrich, R., Haken, H.: Z. Phys. B – Condensed Matter **72**, 265 (1988)
11. Knobloch, E.: Phys. Rev. A**34**, 1538 (1986)
    Deane, A.E., Knobloch, E., Toombre, J.: Phys. Rev. A**36**, 2862 (1987)
    Knobloch, E., Deane, A.E., Toomre, J.: In: Physics of structure and formation: theory and simulation. Güttinger, H., Dangelmayr, G. (eds.). Berlin, Heidelberg, New York: Springer 1987
12. Surko, C.M., Kolodner, P., Passner, A., Walden, R.W.: Physica **23**D, 220 (1986)
13. Brand, H.R., Lomdahl, P.S., Newell, A.C.: Physica D**23**, 345 (1986); Phys. Lett. A**118**, 67 (1986)
14. Coullet, P., Elphik, C., Gil, L., Lega, J.: Phys. Rev. Lett. **59**, 884 (1987)
15. Swift, J., Hohenberg, P.C.: Phys. Rev. A**15**, 319 (1977)
16. Bestehorn, M., Haken, H.: Z. Phys. B – Condensed Matter **57**, 329 (1984)
17. Haken, H.: Synergetics. An introduction. 3rd Edn. Berlin, Heidelberg, New York: Springer 1983

18. Haken, H.: Advanced synergetics. 2. print. Berlin, Heidelberg, New York: Springer 1987
19. Greenside, H.S., Coughran, W.M. Jr.: Phys. Rev. A **30**, 398 (1984)
20. Siggia, E.D., Zippelius, A.: Phys. Rev. Lett. A **47**, 835 (1981)
21. Coullet, P., Elphick, C., Repaux, D.: In: Physics of structure and formation: theory and simulation. Güttinger, H., Dangelmayr, G. (eds.). Berlin, Heidelberg, New York: Springer 1987
22. Ohta, T., Kawasaki, K.: Physica **27**D, 21 (1987)

M. Bestehorn, R. Friedrich, H. Haken
Institut für Theoretische Physik und Synergetik
Universität Stuttgart
Pfaffenwaldring 57/IV
D-7000 Stuttgart 80
Federal Republic of Germany